Spiral Intercellular Calcium Waves in Hippocampal Slice Cultures

MARNI E. HARRIS-WHITE,[1] STEPHEN A. ZANOTTI,[2] SALLY A. FRAUTSCHY,[1] AND ANDREW C. CHARLES[2]

[1]*Department of Medicine, UCLA/Veterans Affairs Medical Center, Sepulveda, CA 91343; and*
[2]*Department of Neurology, UCLA School of Medicine, Los Angeles, California 90095*

Harris-White, Marni E., Stephen A. Zanotti, Sally A. Frautschy, and Andrew C. Charles. Spiral intercellular calcium waves in hippocampal slice cultures. *J. Neurophysiol.* 79: 1045–1052, 1998. Complex patterns of intercellular calcium signaling occur in the CA1 and CA2 regions of hippocampal slice organotypic cultures from neonatal mice. Spontaneous localized intercellular Ca^{2+} waves involving 5–15 cells propagate concentrically from multiple foci in the stratum oriens and s. radiatum. In these same regions, extensive Ca^{2+} waves involving hundreds of cells propagate as curvilinear and spiral wavefronts across broad areas of CA1 and CA2. Ca^{2+} waves travel at rates of 5–10 μm/s, are abolished by thapsigargin, and do not require extracellular Ca^{2+}. Staining for astrocytes and neurons indicates that these intercellular waves occur primarily in astrocytes. The frequency and amplitude of Ca^{2+} waves increase in response to bath application of *N*-methyl-D-aspartate (NMDA) and decrease in response to removal of extracellular Ca^{2+} or application of tetrodotoxin. This novel pattern of intercellular Ca^{2+} signaling is characteristic of the behavior of an excitable medium. Networks of glial cells in the hippocampus may behave as an excitable medium whose spatial and temporal signaling properties are modulated by neuronal activity.

INTRODUCTION

The study of cellular activity in the hippocampus has focused primarily on synaptic neuronal activity. Recently, however, nonsynaptic signaling pathways including glial-glial and bidirectional glial-neuronal signaling have received increasing attention as potential mediators of hippocampal function (Dani et al. 1992; Duffy and MacVicar 1995; Mennerick and Zorumski 1994; Porter and McCarthy 1996; Wu and Barish 1994). These nonsynaptic signaling pathways may modulate traditional synaptic neuronal signaling or play independent roles in the function of the nervous system. Intercellular Ca^{2+} signaling has been observed in hippocampal astrocytes in culture and in hippocampal slice cultures in response to chemical and electrical stimuli (Cornell-Bell et al. 1990; Dani et al. 1992; Duffy and MacVicar 1995). In this study we report novel patterns of organized Ca^{2+} signaling, including spiral waves, involving broad areas of the hippocampus.

Spiral waves are a recurring phenomenon in a wide diversity of natural systems (Block et al. 1996; Davidenko et al. 1992; Siegert and Weijer 1995; Zaritsky et al. 1993). They have been modeled extensively as a characteristic pattern of activity in excitable media (Diks et al. 1995; Steinbock et al. 1993; Winfree 1972). In the *Xenopus* oocyte, spiral waves of increased $[Ca^{2+}]_i$ propagate throughout the cytoplasm; investigation of these waves yielded new insights into the mechanisms of cellular Ca^{2+} signaling (Atri et al. 1993; Lechleiter et al. 1991; Lechleiter and Clapham 1992). We now report intercellular spiral waves in the hippocampus with properties similar to those observed in other systems such as the *Xenopus* oocyte.

METHODS

Hippocampal slice cultures

Hippocampal slice cultures were prepared from 6- to 7-day-old CD-1 mice (Stoppini et al. 1991). Animal care was in accordance with UCLA Animal Research Committee guidelines. Hippocampi were cut into 400-μm sections that were transferred to culture dishes containing Costar membrane inserts (0.4 μm). Slices were then maintained in culture for 2–10 days before experimentation. The culture medium was a mixture of Eagle's minimum essential medium (MEM) + *N*-2-hydroxyethylpiperazine-*N*′-2-ethanesulfonic acid (HEPES; 5%; Gibco), horse serum (25%; Sigma), Hanks' balanced salt solution (25%; Gibco), glucose (6.5 mg/ml), and penicillin-streptomycin (50 U/ml to 0.05 mg/ml), pH 7.2. Slices were maintained in 5% CO_2 in a humidified incubator at 37°. At the time of the experiments, slices had flattened out to 150–200 μm thick, comprising ~10 cell layers. Serial cryostat sections and staining with glial fibrillary acidic protein (GFAP), neuronal cell surface antigen (NCSA), and microtubule associated protein-5 (MAP-5) (see *Immunohistochemistry*) showed that slices maintained normal hippocampal cellular architecture throughout all ages in culture. Only the far edges of the slice thinned out to <10 cell layers; these areas were not imaged. The cellular composition was consistent throughout the thickness of the slice; there was no glial cell layer covering the surface of the slice as verified by cryostat sections.

Experimental procedures

After 2–10 days in culture, slices were submersion loaded in 50 μM fura2-AM (Calbiochem) for 1 h at room temperature in a humidified and oxygenated chamber. The membranes with the slices attached were then excised from the plastic insert, glued to a glass coverslip (ROSS super glue gel was applied around the edge of the membrane; glue hardened immediately on contact with liquid and never contacted the slice) to a glass coverslip, and placed on the stage of a Nikon inverted microscope. Slices were perfused at a rate of 2 ml/min at room temperature that was oxygenated at 95% O_2-5% CO_2 with artificial cerebrospinal fluid (ACFS) containing (in mM) 17 NaCl, 4 KCl, 2.5 $MgSO_4$, 2 $CaCl_2$, 1.25 KH_2PO_4, 10 glucose, 5 $NaHCO_3$, and 20 HEPES, pH 7.2. After fura loading, slices were perfused for 30 min before imaging. For experiments in which O_2 was removed from the perfusion buffer (including 95% N_2-5% CO_2 replacement), the pH was adjusted to 7.2. The pH was constant throughout all experiments. All agonists and antagonists were added to the perfusion medium. Glutamate agonists and antagonists were obtained from Tocris Cooksen. Cul-

ture media was obtained from Cellgro. Unless otherwise specified, all other reagents were obtained from Sigma.

Measurement of $[Ca^{2+}]_i$

$[Ca^{2+}]_i$ was measured with a fluorescence imaging system that was previously described in detail (Charles et al. 1991). Briefly, slices were excited with a mercury lamp through 340- and 380-nm band-pass filters; fluorescence at 510 nm was recorded through a ×20, 0.75 numerical aperture objective on a Nikon Diaphot inverted microscope with a Silicon intensified target camera to an optical memory disk recorder. Images were then digitized and subjected to background subtraction and shading correction, after which $[Ca^{2+}]_i$ was calculated on a pixel-by-pixel basis by a frame grabber and image analysis board (Data Translation) as previously described (Charles et al. 1991). Tracings in Figs. 2*C*, 3*C*, and 4 were based on fluorescence of a 4 × 4 pixel area located within each cell body. Layers of cell bodies within the slice were clearly visualized with the system described, although the resolution was not sufficient to delineate the entire extent of each cell. Background fluorescence was estimated by measuring the fluorescence of an area of the coverslip adjacent to the slice. Slices not loaded with fura showed no fluorescence under our experimental conditions. The entire thickness of the slice appeared to be loaded with fura, and fluorescence from cell bodies of at least three layers of cells could be distinguished in each imaged field as determined by focusing up and down through the field. However, our calculation of $[Ca^{2+}]_i$ did not account for additional out-of-focus and background fluorescence within the slice, and therefore it was possible that actual changes in $[Ca^{2+}]_i$ were greater than those reported. We have reported our measurements as ''estimated $[Ca^{2+}]_i$.''

Neuron cell surface antigen labeling

After fura2 measurements, stage coordinates for the imaged fields were obtained and then slices were removed and treated with antibody to the NCSA (Chemicon; 1/100) for 45 min. Slices were rinsed three times and exposed to a Texas red-tagged secondary antibody for 30 min. The slice was returned to previous image coordinates on the microscope stage and neuronal cell bodies were identified with a rhodamine filter set.

Immunohistochemistry

Slices were fixed in 4% paraformaldehyde fixative for 1 hr and rinsed in phosphate buffered saline. For cryostat sectioning, slices were cryoprotected with sucrose (successive 10, 15, and 20% solutions), sectioned at 10 μm on a Zeiss cryostat, and mounted onto gelatin-coated slides. Slide-mounted whole slices or sections were pretreated with a 0.3% hydrogen peroxide solution (30 min) to block endogenous peroxidase activity and subsequently blocked with a buffer containing bovine serum albumin, Tween20, and a serum appropriate for the particular antibody being used. Slices were incubated with either a GFAP (1:500) or MAP-5 (1:200) antibody for 1 h at room temperature followed by the appropriate biotinylated secondary antibody. Antibody binding was detected with the use of avidin-biotin-peroxidase (ABC Kit, Vector Labs) and the substrate 3,3′-diaminobenzidiene.

RESULTS

The slice explant cultures used for these studies were prepared from 6- to 7-day-old CD-1 mice. These slice explants maintain the characteristic cellular architecture of the hippocampus for up to 2 wk as indicated by phase-contrast microscopy, loading of cells with fura2, and immunolabeling for neurons with MAP-5 and NCSA and for astrocytes with GFAP (Fig. 1 and other data not shown). Labeling for GFAP reveals a complex network of astrocyte cell bodies and processes throughout the slice that is particularly dense in the s. oriens and s. radiatum and more sparse in the pyramidal neuronal layer (Fig. 1). MAP-5 staining reveals neuronal cell bodies primarily in the pyramidal neuronal layer, with some cell bodies and extensive thin dendritic fibers in the s. oriens and straum radiatum. Because our imaging system uses a standard inverted microscope, fura2 fluorescence is collected from multiple vertical layers of cells in each field. We are able to resolve many cell bodies, but not the individual cellular processes that form a complex network throughout the slice. A disadvantage of this limited resolution is the inability to definitively identify individual cells involved in Ca^{2+} signaling. An advantage, however, is the ability to observe patterns of signaling occurring in large fields of cells in multiple planes of the slice.

Organotypic slices exhibit multiple patterns of spontaneous Ca^{2+} *signaling*

Extensive spontaneous Ca^{2+} signaling occurs in these slices without external stimulation. We observe multiple distinct patterns of spontaneous Ca^{2+} signaling in the CA1 and CA2 regions of the hippocampal slice that we characterize as *1*) asynchronous, single-cell oscillations; *2*) small intercellular waves limited to 5–15 cells (Ca^{2+} ''puffs''); and *3*) broad intercellular wavefronts simultaneously involving 50–100 cells that propagate in curvilinear and spiral patterns. Each pattern of signaling was observed in >50 different slice preparations.

Individual cells show rapid, low-amplitude Ca^{2+} oscillations with a period of 5–20 s and an estimated peak $[Ca^{2+}]_i$ of 75–150 nM. These single-cell oscillations are seen throughout CA1 and CA2, but occur most commonly in or immediately adjacent to the pyramidal neuronal cell layer. Small multicellular Ca^{2+} waves (Ca^{2+} puffs) occur frequently from many different sites of initiation in the s. oriens and s. radiatum in CA1 and CA2. These spontaneous Ca^{2+} puffs originate from a single cell (Fig. 2*A*) and spread concentrically at rates of 10–16 m/s to a total of 5–15 cells with estimated Ca^{2+} concentrations ranging from 100 to 200 nM. Although it is not possible to determine whether Ca^{2+} puffs originate in a neuron or involve some neurons, immunostaining for a neuronal marker (NCSA) that labels neurons in the pyramidal neuronal layer (Fig. 1) reveals that the majority of cell bodies participating in the Ca^{2+} puffs are not neurons. Parallel immunostaining for GFAP reveals that Ca^{2+} puffs occur in regions containing many astrocytes (Fig. 1).

In these same regions, broad intercellular wavefronts with a width of 5–10 cells and spanning as many as 100 cells and up to 500 m occur as shown in Fig. 3. Broad intercellular wavefronts are seen spontaneously in ~20% of slices. These intercellular waves may originate in a single cell and propagate in curvilinear and spiral patterns (Fig. 3*A*). The propagation rate of the waves ranges from 5–10 m/s, and the estimated peak $[Ca^{2+}]_i$ amplitude of the wavefront (125–200 nM) is consistent throughout the distance of propagation. In some cases the wavefront passes undiminished

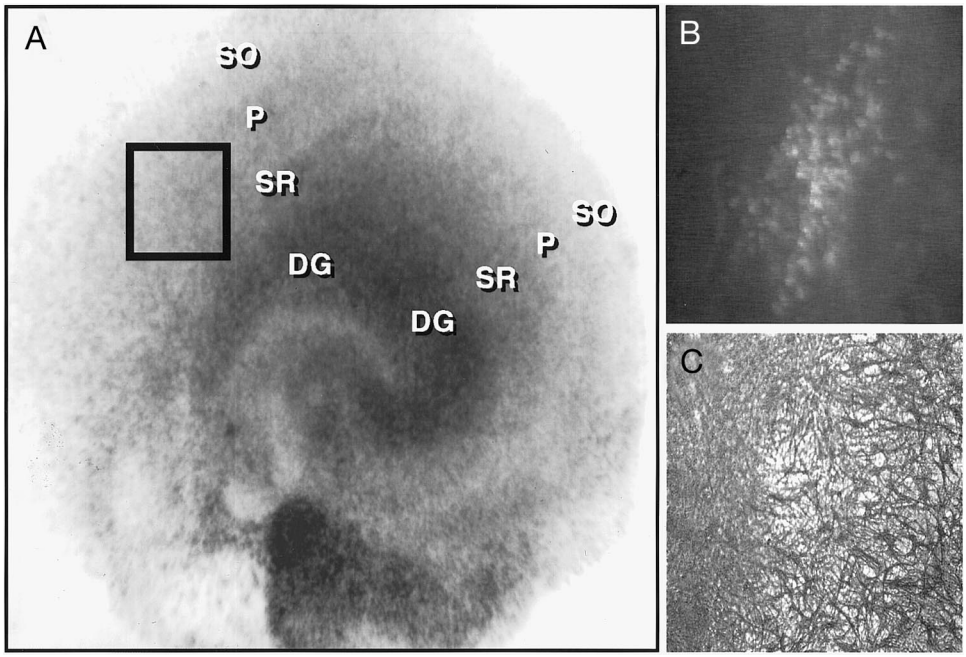

FIG. 1. Typical hippocampal slice organotypic culture. *A*: phase contrast image of a typical hippocampal slice organotypic culture after 4 days in vitro. The box outlines a typical imaged field as represented in *B* and *C* and in Figs. 2 and 3. Scale: 4.5 × 4.5 mm. *B*: neuron cell surface antigen antibody labeling of same region outlined in the box in *A*. Image shows immunofluorescence labeling of pyramidal neurons within a typical imaged field. Scale: 500 μm horizontally × 470 μm vertically. *C*: glial fibrillary acidic protein (GFAP) antibody labeling of a field of cells in the same region of slice. Image shows DAB staining of astrocytes in the CA1 region. Astrocyte cell bodies and processes are more sparse within the neuronal pyramidal layer (*right*) but are densely packed in the stratum oriens (*left*). Scale: 500 μm horizontally × 470 μm vertically. DG, dentate gyrus; SR, s. radiatum; P, pyramidal neuronal layer; SO, s. oriens.

throughout the field of view, whereas in others the wavefront becomes irregular and breaks up as it propagates. When two curvilinear wavefronts collide, they annihilate at the point of contact (Fig. 3*B*). After collision, portions of the waves that have not collided merge and continue to propagate tangentially from the site of collision. The minimum apparent refractory period between waves ranges from 20 to 30 s in different regions of each field of cells (Fig. 3*C*).

Wavefronts most commonly originate in or near the pyramidal neuronal cell layer (CA1–CA2) and travel peripherally through the s. oriens region. However, waves also propagate from the s. radiatum or s. oriens and continue across the pyramidal layer. When these waves encounter the pyramidal neuronal cell layer, there is consistently a change in the temporal and spatial characteristics of propagation. In some cases, Ca^{2+} waves are abolished when they encounter the pyramidal layer, and in other cases there is a delay in propagation of 5–10 s or an interruption in the continuity of the wavefront, after which the wavefront is reestablished on the other side of the pyramidal layer. The alteration of wave propagation at the pyramidal neuronal layer, where there is a decreased density of glial cell bodies, suggests that glial cell-cell contacts are involved in wave propagation.

Wavefronts are initiated periodically from the same 1–5 foci within a 400 × 500 μm field, in contrast to the Ca^{2+} puffs that are initiated nonperiodically from as many as 15 different sites of initiation. As with the Ca^{2+} puffs, it is not possible to determine with certainty whether the spiral waves are initiated by neurons or glia. However, staining for neuronal markers on the same fields reveals that the majority of the cells participating in the waves are not neurons, and parallel staining for GFAP suggests that these cells are astrocytes (Fig. 1).

Ca^{2+} waves do not require extracellular Ca^{2+}

Pharmacological manipulation of the slice provides information regarding mechanisms of Ca^{2+} signaling activity. Replacing the experimental medium with medium containing no added Ca^{2+} and 1 mM ethylene glycol-bis (β-aminoethyl ether)-*N,N,N′,N′*-tetraacetic acid (EGTA) immediately stops most Ca^{2+} oscillations in individual cells (Fig. 4; $n = 9$ slices). The immediate cessation of Ca^{2+} signaling in these cells indicates that extracellular Ca^{2+} ($[Ca^{2+}]_o$) is rapidly and significantly decreased. Ca^{2+} puffs continue for up to 4 min in the absence of $[Ca^{2+}]_o$, although their frequency is reduced. Broad intercellular wavefronts also continue with reduced frequency for up to 4 min following removal of $[Ca^{2+}]_o$ (Fig. 4), after which no further waves are seen. The health of the slices does not appear to be compromised by this treatment, because returning the slices to regular perfusion buffer (containing Ca^{2+}) restores the prior signaling patterns and frequency within 1 min.

Ca^{2+} puffs and wavefronts also continue to occur for ≥4 min in the presence of the nonspecific Ca^{2+} channel blocker Ni^{2+} ($n = 3$ slices, 100 M $NiCl_2$; data not shown), showing that voltage-gated Ca^{2+} channels are not necessary for the propagation of puffs or waves. Both U73122 (20 μM), which inhibits phospholipase C, and thapsigargin (5 μM), which depletes $[Ca^{2+}]_i$ stores, abolish all puffs and spiral waves, consistent with a mechanism involving formation of 3-inositol-1,4,5-trisphosphate (IP_3) and release of Ca^{2+} from intracellular stores ($n = 3$ slices each; data not shown).

Ca^{2+} wave behavior is altered by neuronal activity

The glutamate receptor subtype agonist NMDA has a dramatic effect on the characteristics of Ca^{2+} waves (Fig. 2*B*). Bath application of 20 μM NMDA evokes an immediate, simultaneous increase in $[Ca^{2+}]_i$ in the region identified morphologically as the pyramidal cell layer of CA1. This immediate response is followed in 2–5 s by broad intercellular wavefronts in the s. oriens ($n = 5$ slices) that continue for 1–2 min after application of NMDA. The NMDA–evoked

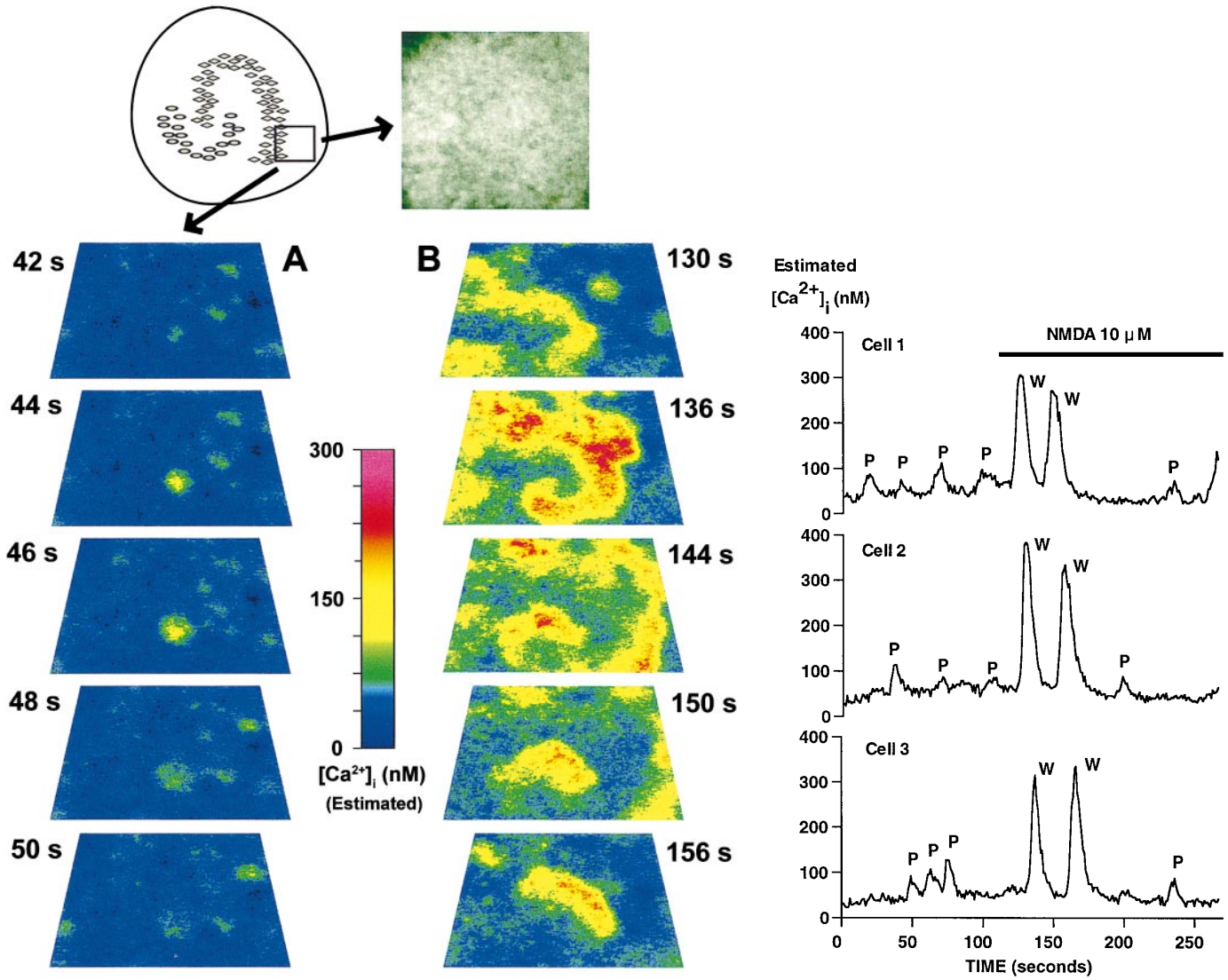

FIG. 2. Spontaneous Ca^{2+} puffs and the response to *N*-methyl-D-aspartate (NMDA). *Top left*: region of the slice explant that is imaged (box). *Top right*: baseline fura2 fluorescence in this region. *A*: spontaneous Ca^{2+} puffs that originate from multiple foci in the s. oriens. *B*: same field 10 s following bath application of 20 μM NMDA. A large spiral wave develops and propagates to involve most cells in the field. Scale: 550 μm horizontally $\times$ 400 μm vertically. *C*: tracings of estimated intracellular Ca^{2+} ($[Ca^{2+}]_i$) vs. time in 3 representative cells in the field shown in *A* and *B*. Spontaneous asynchronous Ca^{2+} puffs occur before addition of NMDA, after which 2 broad intercellular wavefronts pass through all cells. P, Ca^{2+} puffs; W, spiral Ca^{2+} waves.

waves travel faster (10–15 μm/s) and have greater estimated peak $[Ca^{2+}]_i$ (200–300 nM) than spontaneous waves. Because NMDA receptors are generally confined to neurons and are not present on glial cells, these results suggest that stimulation of neurons with NMDA results in a secondary activation of glial Ca^{2+} waves.

One possible mechanism for activation of glial Ca^{2+} signaling by neurons is activation of non-NMDA glutamate receptors by neuronally released glutamate. Consistent with this mechanism, the metabotropic glutamate receptor ($mGlu_r$) antagonist, (±)-methyl-4-carboxyphenylglycine (MCPG; 100 μM), abolishes puffs and waves ($n = 3$ slices; data not shown). Inhibition of neuron-mediated hippocampal astrocytic Ca^{2+} signaling by MCPG was described previously by Porter and McCarthy (1996). However, the $mGlu_r$ agonist *trans*-(±)-1-amino-1,3-cyclopentanedicarboxylic acid (125 μM) has a variable effect, abolishing activity in some instances and having no effect in others ($n = 7$ slices; data not shown). 6,7-Dinitroquinoxaline-2,3-dione (70 μM), a kainate/quisqualate antagonist, *increases* the number of sites of initiation of spiral waves as well as increasing the frequency of the waves, resulting in a more disorganized pattern of activity ($n = 7$ slices; data not shown).

Tetrodotoxin (TTX; 1 μM), which inhibits voltage-gated Na^+ channels and thereby action potentials, has an effect similar to 0 Ca^{2+} ($n = 10$ slices; data not shown). TTX immediately abolishes most single cell Ca^{2+} oscillations, but Ca^{2+} puffs and broad $[Ca^{2+}]_i$ waves continue to occur for $\geq$4 min with reduced frequency.

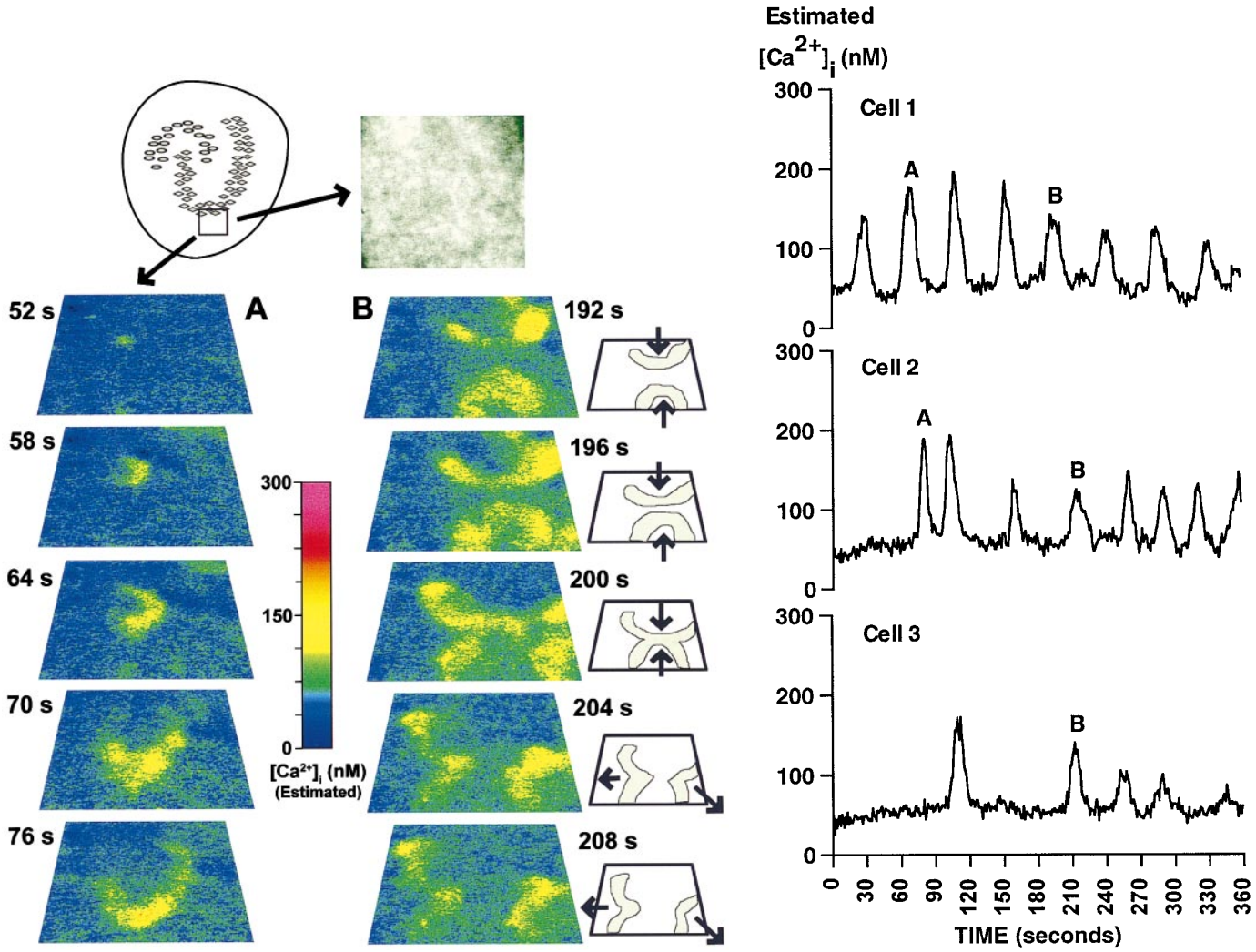

FIG. 3. Spontaneous spiral wave and annihilation of colliding waves. *Top left*: region of the slice explant that is imaged (box). *Top right*: baseline fura2 fluorescence of this region. This slice is an example of the ~2% of slices showing spontaneous broad intercellular wavefronts. *A*: initiation of a spiral intercellular Ca^{2+} wave in a single cell. *B*: same field later in the recording, when 2 curvilinear Ca^{2+} wavefronts collide and annihilate. Arrows in schematic panels to the *right* of *B* indicate direction of propagation of the waves. Scale: 55 μm horizontally × 4 μm vertically. *C*: tracings of estimated $[Ca^{2+}]_i$ vs. time in 3 representative cells in the field. The intercellular waves shown in *A* and *B* are indicated by the letters above the appropriate peak on the tracing. *Cell 1* shows periodic Ca^{2+} waves, whereas *cells 2* and *3* show a less regular pattern of Ca^{2+} wave occurrence.

Oxygen dependence of Ca^{2+} signaling

Removal of O_2 from the perfusion medium results in the immediate cessation of virtually all spontaneous Ca^{2+} oscillations, puffs, and broad intercellular waves ($n = 6$ slices; data not shown). Slices perfused with N_2 purged buffer show no Ca^{2+} signaling for ≥2 min ($n = 3$ slices). After ~2 min of hypoxia Ca^{2+} signaling returns, consisting of all patterns of signaling described in the previous paragraphs. Longer term hypoxia (15–30 min) results in permanent and complete loss of calcium signaling. Control patterns of Ca^{2+} signaling could be recovered following shorter periods of hypoxia (<15 min).

DISCUSSION

These results suggest that Ca^{2+} puffs and wavefronts represent patterns of spontaneous glial intercellular signaling whose frequency, propagation velocity, and amplitude can be altered by neuronal activity. Several characteristics of the Ca^{2+} puffs and waves are consistent with these patterns of signaling occurring primarily in astrocytes. First, the activity occurs with regional specificity in the hippocampus (i.e., it involves cell bodies in the s. radiatum and s. oriens, areas consisting largely of astrocytic cell bodies and processes as demonstrated by GFAP labeling, and fewer neuronal cell bodies and dendrites evidenced by immunabeling with MAP-5 and NCSA). Second, Ca^{2+} waves are delayed or abolished when they encounter the pyramidal neuronal cell layer where there are more neuronal cell bodies and fewer glial cell bodies and processes. Third, the slow rate of propagation of Ca^{2+} puffs and waves (5–15 μm/s) is consistent with the previously described propagation velocity for Ca^{2+} waves in glial cell cultures (Charles et al. 1991; Cornell-Bell et al. 1990).

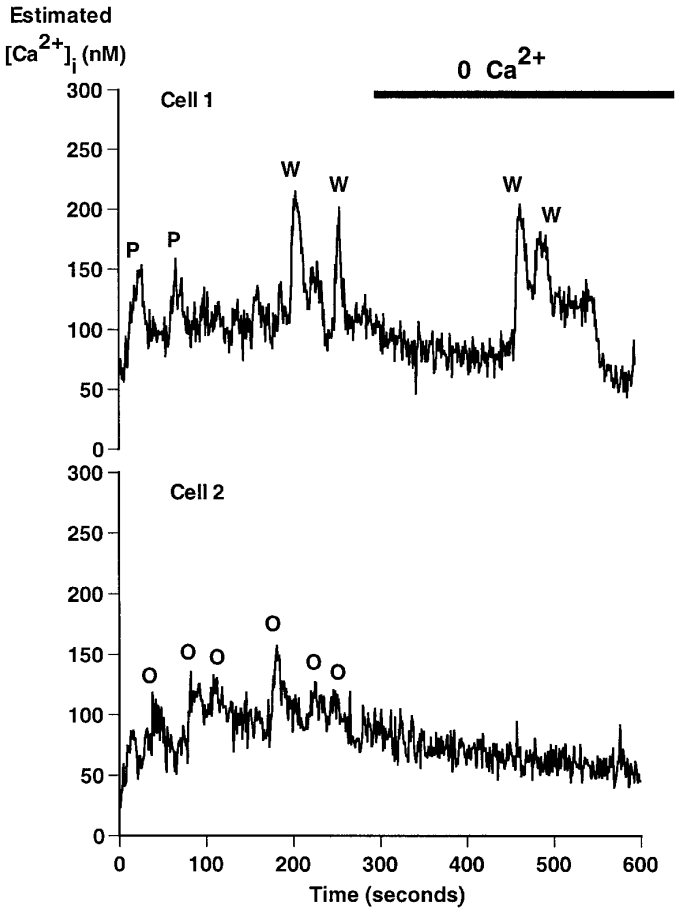

FIG. 4. Effect of removal of extracellular Ca^{2+} ($[Ca^{2+}]_o$). Tracings show estimated $[Ca^{2+}]_i$ vs. time in 2 representative cells before and after replacement of normal experimental medium with medium containing no added Ca^{2+} and 1 mM ethylene glycol-bis(β-aminoethyl ether)-*N*,*N*,*N*′,*N*′-tetraacetic acid. Single cell Ca^{2+} oscillations in *cell 2* are abolished by removal of $[Ca^{2+}]_o$. $[Ca^{2+}]_i$ waves continue in *cell 1* after removal of $[Ca^{2+}]_o$ but their frequency is reduced. O, single-cell Ca^{2+} oscillations; P, Ca^{2+} puffs; W, broad intercellular waves.

Finally, the propagation of the waves via Ca^{2+} release from intracellular stores is also consistent with previously described mechanisms for glial Ca^{2+} signaling (Charles et al. 1993). By contrast, the asynchronous single-cell Ca^{2+} oscillations that occur primarily in the pyramidal neuronal layer and that are abolished by TTX and removal of $[Ca^{2+}]_o$ most likely represent neuronal activity. Similar spontaneous single-cell Ca^{2+} transients were previously described in pyramidal neurons in the immature hippocampal slice (Dailey and Smith 1994).

Spontaneous Ca^{2+} puffs are remarkably similar in their spatial and temporal characteristics to spontaneous glial Ca^{2+} waves observed in mixed glial/neuronal cultures (Charles 1994). However, the broad intercellular wave fronts are significantly different from any previously described patterns of glial Ca^{2+} signaling in culture or slice preparations; these previously reported spontaneous, mechanically-induced, or transmitter-induced glial Ca^{2+} waves (Charles et al. 1991; Charles,1994; Cornell-Bell et al. 1990; Dani et al. 1992; Duffy and MacVicar 1995) do not propagate as wavefronts in curvilinear or spiral patterns.

Potential mechanisms of intercellular Ca^{2+} signaling

The effects of thapsigargin and U73122 on Ca^{2+} puffs and wavefronts are consistent with an Ca^{2+} signaling mechanism involving IP_3-mediated release of Ca^{2+} from intracellular stores. The relatively constant rate of propagation and amplitude of the Ca^{2+} wavefronts over long distances suggest that there is a regenerative mechanism involved in this type of Ca^{2+} signaling. Two possible pathways of propagation of the response from cell-to-cell are gap junctions and the release of a glial extracellular messenger. There is extensive evidence for gap junctional communication as a mechanism for propagation of glial Ca^{2+} waves (Charles et al. 1992; Finkbeiner 1992). In addition, we and others have observed that Ca^{2+} waves in glial cultures can be altered by rapid perfusion of the medium and can cross gaps between cells, suggesting that an extracellular messenger may also be involved (Charles 1997; Hassinger et al. 1996). Parpura et al. (1994) and Jeftinija et al. (1996) provide strong evidence for Ca^{2+}-mediated release of transmitters from glial cells. We favor the hypothesis that a combination of gap junctional communication and Ca^{2+}-dependent release of an extracellular messenger is involved in the intercellular propagation of Ca^{2+} waves.

The O_2 dependence of the spontaneous Ca^{2+} signaling in the slices is consistent with studies showing that acute slice preparations require O_2 perfusion to maintain normal synaptic activity. Schurr et al. (1989) demonstrated that the amplitude of the population spike in an acute hippocampal slice decreased to 0 mV within 2 min of hypoxia induction. Consistent with our findings, they also report that periods of hypoxia lasting >15 min resulted in poor recovery of function. Organotypic slices as prepared in the present study also have similar long-term O_2 requirements as acute slices as indicated by the observation that slices do not survive in culture unless they are maintained at an air-media interface (Stoppini et al. 1991).

The effects of NMDA, TTX, and 0 $[Ca^{2+}]_o$ provide evidence that glial $[Ca^{2+}]_i$ signaling is modulated by neuronal activity. Because glial cells do not generally express NMDA receptors, the immediate and simultaneous increase in $[Ca^{2+}]_i$ evoked by NMDA in the pyramidal neuronal layer of CA1 most likely represents the neuronal response to NMDA, whereas the delayed and sustained propagation of broad intercellular wavefronts in the s. oriens and s. radiatum is consistent with secondary activation of glial signaling. Activation of glial Ca^{2+} signaling by stimulation of neuronal pathways, including application of NMDA, was described previously in hippocampal slice preparations by Dani et al. (1992) and Porter and McCarthy (1996). Although our observations do not eliminate the possibility that NMDA–evoked Ca^{2+} waves may be traveling through neuronal processes, the delayed and sustained propagation of slow waves through regions of the slice that consist primarily of astrocyte cell bodies is more consistent with neuronal activation of glial signaling. Conversely, the reduced frequency of Ca^{2+} puffs and waves under conditions that inhibit neuronal activity (TTX and 0 $[Ca^{2+}]_o$) indicate that although these patterns of intercellular signaling do not require neuronal activity, they are inhibited when neuronal activity is inhibited, consistent with the previous findings of Porter and McCarthy

(1996). The effects of other pharmacological manipulations, particularly the other glutamate receptor agonists and antagonists, are difficult to interpret because we are unable to determine whether the agonists and antagonists are affecting neurons presynaptically or postsynaptically, glially, or all of the above.

Potential functions of intercelluar Ca^{2+} signaling

Although there is significant evidence that neuronal activity modulates glial intercellular signaling in the hippocampal slice, a crucial question is whether the converse is also true, i.e., that intercellular glial Ca^{2+} signaling in turn modulates neuronal activity. Glia-to-neuron signaling has been reported in dissociated culture preparations (Charles 1994; Hassinger et al. 1995; Nedergaard 1994; Parpura et al. 1994). Although we do not as yet have direct evidence for glia-to-neuron signaling in the slice preparation, our observation of broad $[Ca^{2+}]_i$ wavefronts that simultaneously cross over a neuronal layer raises the possibility that these Ca^{2+} wavefronts could temporally and spatially coordinate neuronal activity. Preliminary patch-clamp recordings in these same preparations reveal bursts of action potentials occurring in neurons in the same fields of cells that are displaying $[Ca^{2+}]_i$ waves. Studies are presently underway to determine the relationship of this neuronal bursting activity with Ca^{2+} waves.

CA1 and CA3 pyramidal neurons may display temporal and spatial coordination of discharges, even when there are sparse collateral connections between these neurons (Buzsaki and Chrobak 1995; Buzsaki et al. 1992; Taylor et al. 1995). Taylor et al. (1995) report synchronized oscillations in CA3 neuronal activity at intervals of 24 s mediated by activation of $mGlu_r$s. Although our studies do not involve CA3, this temporal, spatial, and pharmacological pattern of neuronal synchronization is consistent with the patterns of intercellular signaling we report here, suggesting that broad glial wavefronts could be involved in neuronal synchronization in the hippocampus. In addition, because broad glial wavefronts continue in the absence of $[Ca^{2+}]_o$, it is possible that glial intercellular signaling plays a role in the nonsynaptic synchronization of neuronal activity in the hippocampus that has been observed in low $[Ca^{2+}]_o$ (Hochman et al. 1995; Jefferys and Haas 1982; Taylor and Dudek 1984). Support for a glial role in the coordination of neuronal activity in the hippocampus is provided by the observation of a close relationship between the magnitude of glial depolarizations and simultaneously recorded field potentials in rat hippocampal slices during 4-aminopyridine–induced synchronous activity (Avoli et al. 1993).

Because these studies were performed with immature hippocampal slices, another possibility is that the patterns of Ca^{2+} signaling reported here are involved in the development of the functional cellular architecture of the hippocampus, as has been suggested for multicellular Ca^{2+} signaling observed in cortical slice preparations (Kandler and Katz 1995; Yuste et al. 1995). Ca^{2+} puffs in the hippocampus have similar spatial and pharmacological properties as Ca^{2+} waves (Kandler and Katz 1995; Yuste et al. 1995) in cortical slices of postnatal rats. Aniksztejn et al. (1995) reported current oscillations induced by metabotropic receptors in immature rat CA3 hippocampal neurons; these current oscillations have similar temporal and pharmacological properties to the intercellular signaling we report here.

Comparison with Ca^{2+} signaling in other preparations

Intercellular Ca^{2+} signaling was reported previously in astrocytes in hippocampal slice preparations (Dani et al. 1992; Duffy and MacVicar 1995). However, this signaling does not occur in organized wavefronts with clear periodicity and refractory periods, and spiral waves were not observed. Spiral intercellular waves of depolarization were reported in cardiac muscle (Davidenko et al. 1992). Significant differences between spiral waves in cardiac muscle and those reported here include a much faster rate of propagation in cardiac muscle, the propagation of a depolarization rather than a change in $[Ca^{2+}]_i$, and the relatively uniform cellular composition of the heart compared with the heterogeneous cellular composition of the hippocampus.

Spreading depression (SD) is a slowly propagating depression of neuronal activity and transmembrane ionic gradients arising in vertebrate gray matter (Leao 1944). Spiral waves of SD have been reported in the intact retina (Gorelova and Bures 1983). Waves of SD in the retina have several features in common with spiral calcium waves in hippocampal slice cultures. Waves of SD propagate at rates of 18–60 μm/s (Gorelova and Bures 1983; Nedergaard et al. 1995; Shibata and Bures 1974), which are similar to the rates of 5–15 μm/s we report here. Both retinal SD and hippocampal Ca^{2+} waves display refractory periods and annhilation of waves on collision (Gorelova and Bures 1983), and both occur in a heterogeneous cellular environment involving the participation of neurons and astrocytes (Fernandes de Lima et al. 1993; Nedergaard et al. 1995).

There are several features of Ca^{2+} signaling within *Xenopus laevis* oocytes that are similar to those seen between cells in hippocampal slice explants. Oocytes also display multiple patterns of increased Ca^{2+} signaling including focal increases in $[Ca^{2+}]_i$, Ca^{2+} oscillations, and propagating planar and spiral wavefronts that annihilate on collision (Lechleiter et al. 1991). In oocytes the rate of propagation of Ca^{2+} waves is 10–30 μm/s, whereas in hippocampal slices it is 5–15 μm/s. In oocytes the refractory period beween Ca^{2+} waves is 4.7 s, whereas in hippocampal slices it is 20–30 s. In both preparations, the Ca^{2+} waves are primarily mediated by release of Ca^{2+} from intracellular stores. The major difference in the pattern of signaling in the two preparations is that the structure of the wavefront is less uniform in the brain slice than in the oocyte. This difference is likely due in large part to the heterogeneous multicellular composition of the slice and variability in the propagation of the response from cell to cell.

Spiral waves have been identified as a characteristic behavior of excitable media (Diks et al. 1995; Steinbock et al. 1993; Winfree 1972). The patterns of intercellular signaling we observe in hippocampal slice explants are similar to patterns of signal propagation observed in a number of other systems that have been modeled as excitable media (Davidenko et al. 1992; Lechleiter et al. 1991; Siegert and Weijer 1995). Modeling of spiral wave behavior in other systems may therefore have applications to intercellular signaling in the brain. Our studies raise the possibility that networks of

glial cells behave as an excitable medium that responds to neuronal input and that the behavior of this medium plays a role in temporal and spatial coordination of activity in the hippocampus.

We thank Drs. James Sneyd and Scott Boitano for helpful comments. Data acquisition and analysis software were written by Dr. Michael Sanderson.

This work was supported by a Turken Foundation Fellowship and a French Foundation Fellowship to M. E. Harris and National Institute of Neurological Disorders and Stroke Grants R29-NS-32283 and P1-NS-2808 to A. C. Charles and R01-NS-3195 to S. A. Frautschy.

Address for reprint requests: A. Charles, UCLA Dept. of Neurology, 710 Westwood Plaza, Los Angeles, CA 90095.

Received 15 July 1997; accepted in final form 14 October 1997.

REFERENCES

ANIKSZTEJN, L., SCIANCALEPORE, M., BEN-ARI, Y., AND CHERJBINI, E. Persistent current oscilllations produced by activation of metabotropic glutamate receptors in immature rat CA3 hippocampal neurons. *J Neurophysiol*. 73: 1422–1429, 1995.

ATRI, A., AMUNDSON, J., CLAPHAM, D., AND SNEYD, J. A single-pool model for intracellular calcium oscillations and waves in the *Xenopus laevis* oocyte. *Biophys. J*. 65: 1727–1739, 1993.

AVOLI, M., PSARROPOULOU, C., TANCREDI, V., AND FUETA, Y. On the synchronous activity induced by 4-aminopyridine in the CA3 subfield of juvenile rat hippocampus. *J. Neurophysiol.* 7: 1018–1029, 1993.

BLOCK, D. L., ELMEGREEN, B. G., AND WAINSCOTT, R. J. Smooth dark spiral arms in the flocculent galaxy NGC2841. *Nature* 381: 674–676, 1996.

BUZSAKI, G. AND CHROBAK, J. J. Temporal structure in spatially organized neuronal ensembles: a role for interneuronal networks. *Curr. Opin. Neurobiol.* 5: 504–510, 1995.

BUZSAKI, G., HORVATH, Z., URIOSTE, R., HETKE, J., AND WISE, K. High-frequency network oscillation in the hippocampus. *Science* 256: 1025–1027, 1992.

CHARLES, A. C. Glia-neuron intercellular calcium signaling. *Dev. Neurosci.* 16: 196–206, 1994.

CHARLES, A. C. Intercellular calcium waves in glia. *Glia*. In press.

CHARLES, A. C., DIRKSEN, E. R., MERRILL, J. E., AND SANDERSON, M. J. Mechanisms of intercellular calcium signaling in glial cells studied with dantrolene and thapsigargin. *Glia* 7: 134–145, 1993.

CHARLES, A. C., MERRILL, J. E., DIRKSEN, E. R., AND SANDERSON, M. J. Intercellular signaling in glial cells: calcium waves and oscillations in response to mechanical stimulation and glutamate. *Neuron* 6: 983–992, 1991.

CHARLES, A. C., NAUS, C. C., ZHU, D., KIDDER, G. M., DIRKSEN, E. R., AND SANDERSON, M. J. Intercellular calcium signaling via gap junctions in glioma cells. *J. Cell Biol.* 118: 195–201, 1992.

CORNELL-BELL, A. H., FINKBEINER, S. M., COOPER, M. S., AND SMITH, S. J. Glutamate induces calcium waves in cultured astrocytes: long-range glial signaling. *Science* 247: 470–473, 199.

DAILEY, M. E. AND SMITH, S. J. Spontaneous Ca^{2+} transients in developing hippocampal pyramidal cells. *J. Neurobiol.* 25: 243–251, 1994.

DANI, J. W., CHERNJAVSKY, A., AND SMITH, S. J. Neuronal activity triggers calcium waves in hippocampal astrocyte networks. *Neuron* 8: 429–440, 1992.

DAVIDENKO, J. M., PERTSOV, A. M., SALOMONSZ, R., BAXTER, W. P., AND JALIFE, J. Spatiotemporal irregularities of spiral wave activity in isolated ventricular muscle. *J. Electrocardiol*. 24, *Suppl*: 113–122, 1992.

DIKS, C., HOEKSTRA, B., AND DEGOEDE, J. Spiral wave dynamics. *Chaos Solitons and Fractals* 5: 645–660, 1995.

DUFFY, S. AND MACVICAR, B. A. Adrenergic calcium signaling in astrocyte networks within the hippocampal slice. *J. Neurosci.* 15: 5535–5550, 1995.

FERNANDES DE LIMA, V. M., SCHELLER, D., HANKE, W., AND SCHLUE, W. R. Self-sustained depressions in the chick retina and short-term neuronal-glial interactions within the gray matter neuropil. *Brain Res*. 614: 45–51, 1993.

FINKBEINER, S. Calcium waves in astrocytes-filling in the gaps. *Neuron* 8: 1101–1118, 1992.

GORELOVA, N. A. AND BURES, J. Spiral waves of spreading depression in the isolated chick retina. *J. Neurobiol.* 14: 353–363, 1983.

HASSINGER, T. D., ATKINSON, P. B., STRECKER, G. J., WHALEN, L. R., DUDEK, F. E., KOSSEL, A. H., AND KATER, S. B. Evidence for glutamate-mediated activation of hippocampal neurons by glial calcium waves. *J. Neurobiol.* 28: 159–170, 1995.

HASSINGER, T. D., GUTHRIE, P. B., ATKINSON, P. B., BENNETT, M. V., AND KATER, S. B. An extracellular signaling component in propagation of astrocytic calcium waves. *Proc. Natl. Acad. Sci. USA* 93: 13268–13273, 1996.

HOCHMAN, D. W., BARABAN, S. C., OWENS, J. W., AND SCHWARTZKROIN, P. A. Dissociation of synchronization and excitability in furosemide blockade of epileptiform activity. *Science* 270: 99–102, 1995.

JEFFERYS, J. G. AND HAAS, H. L. Synchronized bursting of CA1 hippocampal pyramidal cells in the absence of synaptic transmission. *Nature* 300: 448–450, 1982.

JEFTINIJA, S. D., JEFTINIJA, K. V., STEFANOVIC, G., AND LIU, F. Neuroligand-evoked calcium-dependent release of excitatory amino acids from cultured astrocytes. *J. Neurochem*. 66: 676–684, 1996.

KANDLER, K. AND KATZ, L. C. Neuronal coupling and uncoupling in the developing nervous system. *Curr. Opin. Neurobiol.* 5: 98–105, 1995.

LEAO, A. Spreading depression of activity in cerebral cortex. *J. Neurophysiol.* 7: 359–390, 1944.

LECHLEITER, J., GIRARD, S., PERALTA, E., AND CLAPHAM, D. Spiral calcium wave propagation and annihilation in *Xenopus laevis* oocytes. *Science* 252: 123–126, 1991.

LECHLEITER, J. D. AND CLAPHAM, D. E. Molecular mechanisms of intracellular calcium excitability in *X. laevis* oocytes. *Cell* 69: 283–294, 1992.

MENNERICK, S. AND ZORUMSKI, C. F. Glial contributions to excitatory neurotransmission in cultured hippocampal cells. *Nature* 368: 59–62, 1994.

NEDERGAARD, M. Direct signaling from astrocytes to neurons in cultures of mammalian brain cells. *Science* 263: 1768–1771, 1994.

NEDERGAARD, M., COOPER, A.J.L., AND GOLDMAN, S. A. Gap junctions are required for the propagation of spreading depression. *J. Neurobiol.* 28: 433–444, 1995.

PARPURA, V., BASARSKY, T. A., LIU, F., JEFTINIJA, K., JEFTINIJA, S., AND HAYDON, P. G. Glutamate-mediated astrocyte-neuron signalling. *Nature* 369: 744–747, 1994.

PORTER, J. T. AND MCCARTHY, K. D. Hippocampal astrocytes in situ respond to glutamate released from synaptic terminals. *J. Neurosci.* 16: 5073–5081, 1996.

SCHURR, A., WEST, C. A., AND RIGOR, B. M. Electrophysiology of energy metabolism and neuronal function in the hippocampal slice preparation. *J. Neurosci. Methods* 28: 7–13, 1989.

SHIBATA, M. AND BURES, J. Optimum topographical conditions for reverberating cortical spreading depression in rats. *J. Neurobiol.* 5: 107–118, 1974.

SIEGERT, F. AND WEIJER, C. J. Spiral and concentric waves organize multicellular dictyostelium mounds. *Curr. Biol.* 5: 937–943, 1995.

STEINBOCK, O., ZYKOV, V., AND MULLER, S. C. Control of spiral wave dynamics in active media by periodic modulation of excitability. *Nature* 366: 322–324, 1993.

STOPPINI, L., BUCHS, P. A., AND MULLER, D. A simple method for organotypic cultures of nervous tissue. *J. Neurosci. Methods* 37: 173–182, 1991.

TAYLOR, C. P. AND DUDEK, F. E. Synchronization without active chemical synapses during hippocampal afterdischarges. *J. Neurophysiol.* 52: 143–155, 1984.

TAYLOR, G. W., MERLIN, L. R., AND WONG, R. K. Synchronized oscillations in hippocampal CA3 neurons induced by metabotropic glutamate receptor activation. *J. Neurosci.* 15: 8039–8052, 1995.

WINFREE, A. T. Spiral waves of chemical activity. *Science* 175: 634–636, 1972.

WU, R. L. AND BARISH, M. E. Astroglial modulation of transient potassium current development in cultured mouse hippocampal neurons. *J. Neurosci.* 14: 1677–1687, 1994.

YUSTE, R., NELSON, D. A., RUBIN, W. W., AND KATZ, L. C. Neuronal domains in developing neocortex: mechanisms of coactivation. *Neuron* 14: 7–17, 1995.

ZARITSKY, D., RIX, H. W., AND RIEKE, M. Inner spiral stucture of the galaxy M51. *Nature* 364: 313–315, 1993.